Amplified spontaneous emission in high-power burst-mode fiber lasers

S. Yilmaz,[1] P. Elahi,[1,*] H. Kalaycıoğlu,[1] and F. Ömer Ilday[1,2]

[1]Department of Physics, Bilkent University, Ankara 06800, Turkey
[2]Department of Electrical and Electronics Engineering, Bilkent University, Ankara 06800, Turkey
*Corresponding author: pelahi@fen.bilkent.edu.tr

Burst-mode operation of ultrafast lasers is drawing much attention due to its substantial advantages in material processing, particularly in terms of ablation rates and efficiency. However, development of burst-mode lasers is in its infancy and in particular, fiber lasers that have been reported to date have operated at relatively low powers until recently. An important limitation arises from amplified spontaneous emission generation between the pulse bursts, which needs to be better understood. We report a detailed characterization of amplified spontaneous emission generation in a high-power, continuously pumped Yb-doped fiber laser. The laser system implements doping management for balanced mitigation of thermal and nonlinear effects. Furthermore, we present generation of pulse bursts with an average power as much as 145 W, which is the highest power generated from a burst-mode fiber laser, to the best of our knowledge. The average pulse energy is 14.5 μJ at 1 MHz. Pulses of 13 ps are generated directly from the laser without requiring external compression. © 2015 Optical Society of America

1. INTRODUCTION

There is strong interest in the development of ultrafast fiber laser systems providing high-power femtosecond or picosecond pulses increasingly for use in applications outside of a research laboratory [1,2]. In particular, the ultrafast laser serves as an advanced tool for material processing with greatly reduced or absent heat effects [3] in the fabrication of miniaturized devices, precision micromachining [4], self-assembly techniques, highly controlled surface texturing [5], and pulsed laser deposition of high-quality films. The benefits of ultrashort pulses are realized when the laser pulse duration is comparable to or shorter than the electron–phonon thermal coupling time of the material of interest [6]. There is an ongoing debate on how short pulses need to be to benefit from this regime. While this condition is truly fulfilled in the femtosecond regime, for many materials and especially for metals, most of the benefits are evidently obtained with pulse durations up to 10 ps [6]. This assumes that each laser pulse is placed on the material spatially and temporally such that no major amount of heat buildup occurs [7]. In contrast, soft materials, such as tissue, require much shorter pulses, but such targets are not compatible with high average powers, as considered here. In addition to the operational complexity and high cost of ultrafast laser systems, which can successfully be addressed by fiber

lasers, perhaps the most important obstacle to their widespread use in micromachining is the limited ablation speed, in addition to the high energies required, which render the laser system complicated. The benefits of simply scaling up the repetition rate are limited by the finite speeds of beam positioning devices, such as galvanometric scanners. A very interesting and until recently underappreciated technique is to generate bursts of high-repetition-rate pulses at a lower overall repetition rate [8]. This way, the ablation efficiency per pulse has been predicted to scale up by almost an order of magnitude [9]. Furthermore, the lower repetition rate for the bursts allows the beam to be repositioned in time using existing technology. However, most of the burst-mode advances have been demonstrated using solid state lasers, which lack much of the practical advantages offered by fiber lasers. Recently, Kalaycıoğlu and co-workers have demonstrated the first high-energy burst-mode fiber laser and developed it [10–12]. Breitkopf *et al.* reported on a lower-repetition-rate, higher-burst-energy fiber laser [13]. These lasers were pumped with laser diodes pulsing in synchrony to the bursts to minimize amplified spontaneous emission (ASE), which complicates the laser setup. Thus, it is important both scientifically and in terms of practical development of ultrafast burst-mode lasers to better understand and characterize the limitations from ASE buildup between bursts.

Here, we report a detailed characterization of the burst repetition rate and associated ASE generation that can be achieved under continuous pumping. ASE generation is monitored directly in a special time-gating measurement setup. Other methods for ASE measurement have been reported in [14]. To measure ASE, the laser system generates bursts with average power of 50 W. The bursts contain between 10 and 125 pulses with burst repetition rates between 1 MHz and 80 kHz, while keeping the average pulse energy at 5 µJ. We find that pulsed pumping is not required at burst repetition rates above 200 kHz to maintain an ASE ratio of less than 2%. Based on these results, we scaled output power up to 145 W for 1 MHz burst repetition rates comprised of 10 pulses inside the burst. The pulse duration is estimated to be 13 ps, representing ~1.5-fold and 1.9-fold in average power and peak power, respectively, as well as a 30% reduction in pulse duration, compared to our previous results [15]. The estimated ASE ratio is less than 2%. These constitute the highest average power results for any ultrafast burst-mode laser, to the best of our knowledge.

2. EXPERIMENTAL SETUP

The experimental setup is summarized in Fig. 1 and is similar to that described in [15]. A five-stage laser amplifier is seeded from a mode-locked fiber oscillator [16], supplying 13 mW, 3.6 ps long chirped pulses through its fiber port. The spectral bandwidth is 9 nm, centered at 1034 nm. The repetition rate of the oscillator is chosen to be 100 MHz, which is high enough to benefit from increased efficiency during burst-mode operation [9]. A fiber-coupled acousto-optic modulator (AOM) is used to impress the envelope that defines the pulse bursts. Each burst contains an adjustable number of pulses, ranging from 10 to 125 pulses per burst, depending on the burst repetition rate, such that individual pulse energy is kept constant.

The pulses are first stretched to 41 ps in a 120 m long standard single-mode fiber. The first and second amplifier stages comprise core-pumped Yb-doped fibers (40 cm long with

500 dB/m absorption at 976 nm and 15 cm long with 1200 dB/m absorption at 976 nm, respectively) with a 6 µm core diameter. A single-pump diode is used, splitting its output by 30% and 70% to pump the first and second stages, respectively. The amplified power is 150 mW. This is followed by an inline isolator. The third state comprises a 140 cm long double-clad (DC) Yb-fiber with a 20 µm core diameter and 125 µm for the cladding diameter (29 dB/m cladding absorption at 976 nm). A 2-port pump-signal combiner is used to launch a pump power of 16 W from a multimode diode laser, which is temperature stabilized to operate at 976 nm. The signal pump is thus increased to 11 W. Given the complexity of grating-based compression beyond roughly 100 W of average power, we implemented the approach demonstrated in [15], namely, negatively prechirping the pulses prior to launching into the power amplifier, generating chirped, ~10 ps pulses directly. Coupling to the power amplifier is achieved with a fiber-pigtailed collimator with a lead fiber of 20 µm core diameter. The high-power amplifier is the most challenging part of the system. Nonlinear effects and thermal effects limiting the achievable peak and average power levels, respectively. Therefore, we designed this section as composed of two power amplifier stages. The first power amplifier, and fourth overall stage of the setup, utilizes a 2.8 m long DC Yb-doped fiber with a 25 µm core diameter and a 250 µm cladding diameter with 6.5 dB/m cladding absorption at 976 nm. This stage is pumped by two 25 W pump diodes (Oclaro, Inc.), delivered through a 2-port pump-signal combiner. The launched signal is 3.8 W and the output power is 34 W. The measured slope efficiency is 70%. The fifth and final stage implements discrete doping management using a combination of high-doped and low-doped fibers [17]. The low-doped first section is the same fiber as used in stage four with identical core and cladding diameters. The high-doped fiber has also the same core and cladding diameters, but its cladding absorption is 10.8 dB/m. The relative lengths of the two fibers (1 m of low-doped fiber, followed by 2.7 m of high-doped fiber) were determined, first coarsely through numerical simulations, using an improved version of the model reported in [18] and fine-tuned experimentally. A 6-port pump-signal combined is used to deliver pump light from six diode lasers. The diodes are temperature stabilized to operate at around 976 nm.

3. RESULTS AND DISCUSSION

In order to optimize the laser system, it is essential to understand the limitations on burst-mode parameters arising from the laser dynamics, including the important limitation imposed by ASE generation. To fully exploit the benefits of the ultrafast burst mode, the repetition rate of the pulses comprising the bursts should be at least tens of MHz and preferably higher. Then, due to the short durations between pulses inside the burst, pumping during bursts cannot substantially repopulate the upper state of the gain medium, which implies that virtually all of the pump energy has to be delivered and stored in the gain medium during the intermission between subsequent bursts. ASE generation between the bursts not only depletes the population inversion, reducing gain available for the bursts upon their arrival, but only generates spurious quasi-CW emission,
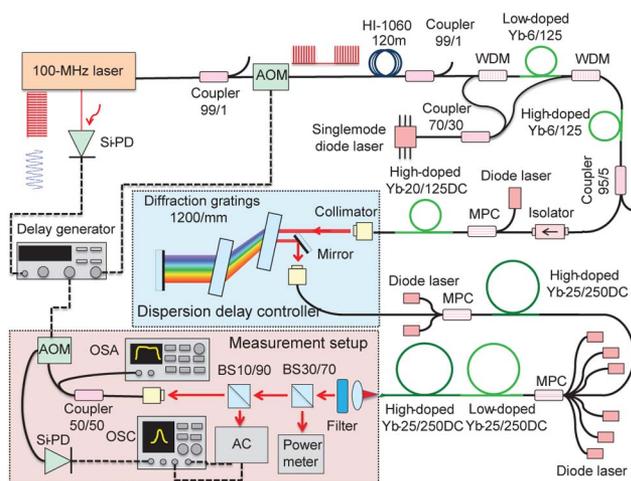
Fig. 1. Schematic diagram of the setup. AOM, acousto-optic modulator; WDM, wavelength-division multiplexer; MPC, multiple pump-signal combiner; Si-PD, silicon photodetector; AC, autocorrelator; OSA, optical spectrum analyzer; OSC, oscilloscope.

filling in between the bursts. The ASE generated in the first amplifier is amplified in the next stage and generates more.

The ASE is amplified proportional to the gain generated in the first amplifier addition. Since ASE is generated in both directions, the component of ASE propagating in the direction opposite to that of the pulses can cause heating-related damage to earlier amplifier stages or lead to detrimental giant pulse formation. These possibilities have particularly serious implications in the kHz repetition rates, unless synchronously pulsed pumping is utilized. Furthermore, with increasing stored energies, the first few pulses of the burst deplete much of the gain at low repetition rates, leading to significant energy variations across the burst [11].

A. Burst Characterization and ASE Measurement

To characterize burst dynamics, we implemented a measurement setup which enables us to investigate the detailed system characteristics simultaneously, as well as measure ASE content directly in the time domain as first described in [19]. Figure 1 depicts the measurement setup. Output of the gain fiber of final amplifier stage is angle-cleaved to prevent back-reflected light from getting coupled back into the core. After collimating the beam, residual pump light is filtered out with a dichroic mirror. For autocorrelation and optical spectrum measurements, power is decreased with a nonpolarizing 70%/30% beam splitter. The larger portion is sent to a power meter for continuous monitoring. The smaller portion is passed through a second, nonpolarizing 90%/10% beam splitter, sending its smaller portion to the autocorrelator and the larger portion to a fiber collimator. The fiber-coupled light is further split into two equal arms with a fiber coupler for optical spectrum and ASE measurements. The ASE measurements are performed by passing the light through a second AOM, which is gated with the negative of the signal applied to the first AOM with a properly adjusted delay. The resulting action is to drop the burst signal, such that any (ASE) signal between the bursts is easily detectable with a sensitive power meter. Further details can be found in [19]. Since the presence of a substantial amount of ASE signal not only limits the achievable pulse energy but can also lead to catastrophic damage to the laser system, utmost care was taken during the ASE characterizations. As a precaution, the output power was limited to 50 W. In order to rule out any indirect influence of nonlinear effects on the ASE measurements, which could occur due to, e.g., changes in efficiency due to Raman-induced redshifting of the spectrum, the (average) pulse energy was kept constant (5 µJ). This was achieved by adjusting the number of pulses per burst to between 10 and 125, corresponding to burst energies ranging from 50 to 625 µJ and burst repetition rates ranging from 1 MHz to 80 kHz, respectively.

The pulse burst generated from the power amplifier is shown in Fig. 2(a) for a 1 MHz burst repetition rate which corresponds to 10 pulses inside the one burst. Depletion of the gain during the burst is considerable, which results in significant variation in pulse energy across the burst. In particular, when the time delay between two bursts is increased (the burst repetition rate is decreased), the variation becomes significant [Figs. 2(b) and 2(c)]. Figure 2(d) shows the measured pulse energy variation across the burst for different burst repetition
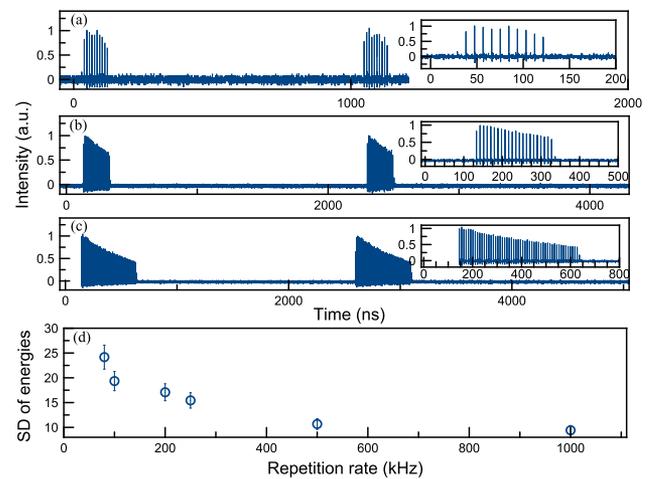

Fig. 2. Measured temporal profile of the pulse burst at 50 W output power. Inset: close-up showing the pulse train at repetition rates of (a) 1 MHz, (b) 500 kHz, and (c) 200 kHz. (d) Standard deviation (SD) of pulse energies within the pulse bursts as a function of burst repetition rate measured at 50 W.

rates. This variation can be compensated for by preshaping the burst envelope [11] at the cost of increased complexity in control electronics. However, at burst repetition rates above 500 kHz, the standard deviation of the pulse energy within a burst is less than ~10% [Fig. 2(d)]. In this work, preshaping is not utilized for the sake of simplicity. Experimental measurements demonstrate that ASE between bursts rises sharply for burst repetition rates below 200 kHz [Fig. 3(a)]. However, the fractional amount of energy within the ASE signal remains in the range of a benign and acceptable level of 1% for burst repetition rates of 200 kHz and higher.

B. Optimization and Power Scaling

Having determined the dependence of ASE levels and pulse-to-pulse energy variations as a function of the burst repetition rate, we have optimized the system for high-power operation. At a burst repetition rate of 1 MHz, ASE ceases to be a limiting factor. The laser system generates 100 ns long bursts, containing 10 pulses each. The maximum average power is 145 W, limited by available pump power, and the slope efficiency is ~70% [Fig. 4(a)].

Figure 4(b) shows the measured optical spectrum for 50, 100, and 145 W output power, corresponding to 5, 10, and 14.5 µJ of individual pulse energies, respectively. As the pulse
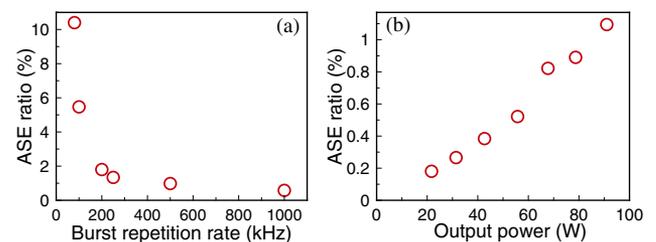
Fig. 3. (a) Measured ASE/output power ratio as a function of burst repetition rate at 50 W output. (b) Measured ASE/output power ratio versus output power, for which the burst repetition rate was kept at 1 MHz.
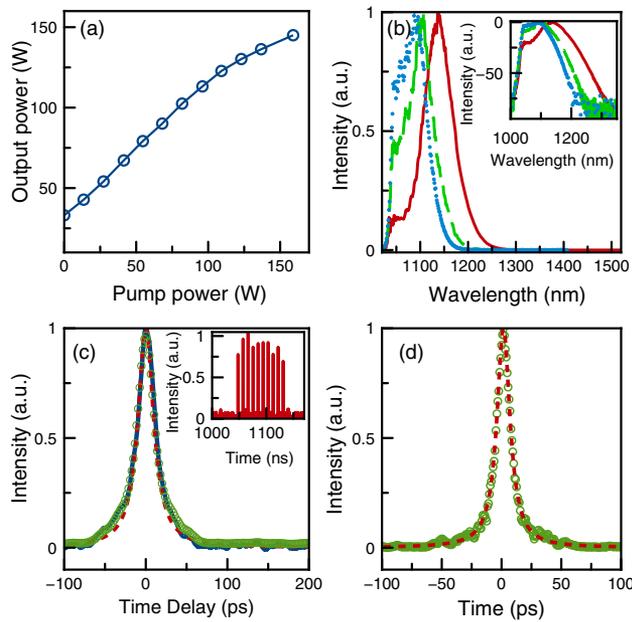
Fig. 4. (a) Measured output power versus pump power. (b) Measured output spectra in burst-mode operation at output powers of 50 W (blue dotted line), 100 W (green dashed line), and 145 W (red solid line) shown as linear and in the inset as semi-log plots. (c) Measured intensity autocorrelation at 145 W of output power (blue solid line) along with the retrieved autocorrelation trace obtained using PICASO (green circles) and Lorentzian fit (red dashed line). Inset: pulse train in one burst from the power amplifier at 145 W output power. (d) Retrieved pulse shape (green circles) and Lorentzian fit (red dashed line) with FWHM of 12 ps.

energy is increased, four-wave mixing and intrapulse Raman scattering lead to spectral broadening and redshifting substantially beyond the gain bandwidth. However, gain narrowing ultimately limits the spectral width to 70 nm. The average energy for the pulses within the burst is 14.5 µJ. The variation of energy in the burst is calculated to be 9%. The measured autocorrelation signal is presented in Fig. 4(c), fitted by a Lorentzian pulse intensity shape, which provides a better fit than the commonly used Gaussian shape. The inferred full width at half-maximum (FWHM) pulse duration is 12.8 ps. We also used the PICASO algorithm [20] to fit the measured autocorrelation and optical spectrum with an arbitrary spectral phase profile, from which the inferred FWHM pulse duration was 12 ps. We note that while this retrieval procedure [Fig. 4(d)] cannot predict the pulse shape accurately, it gives an arguably more reliable estimate of the pulse duration than simply fitting the autocorrelation trace with a fixed pulse shape. However, the results should be considered as a replacement for proper pulse retrieval.

At the highest power of 145 W, the estimated nonlinear phase shift in the last stage of amplification is about 180π. The resulting spectral evolution is dominated by Raman scattering, as evidenced by the asymmetric growth of the spectrum toward longer wavelengths. However, there is a complex interplay between Raman scattering, SPM, and higher-order dispersion. Soliton-like effects that typically underlie similar spectral enhancements do not play a significant role since

the fibers have normal dispersion and the pulses are positively chirped in the regions where nonlinearity is the strongest. As expected, there is a trade-off between nonlinear spectral reshaping and pulse duration, similar to the results in [17]. If the launched pulses are more heavily chirped, nonlinear effects are reduced, but this results in longer pulses. For shorter launched pulse durations, nonlinear spectral broadening leads to additional dispersive stretching. Thus, the pulse duration becomes clamped. However, by implementing doping management with a third segment with an even higher doping level (increasing the gain/length), gain filtering can be exploited to reduce pulse durations to sub-10 ps.

4. CONCLUSIONS

In conclusion, we have carried out systemic investigations of ASE generation for a burst-mode fiber laser system using a direct, time-domain measurement system. Our results indicate that pulsed pumping employed in [10–12] is not required as long as bursts are repeated at 200 kHz or higher for 50 W operation, which allows for substantial simplification of the setup. Even lower repetition rates would be possible at lower average powers. In addition, preshaping of the pulse energies within the burst in order to decrease the pulse-to-pulse energy variations is not needed for high burst repetition rate cases, which further simplifies the electronics of the setup. Based on this analysis, we have constructed a fiber laser system operating in the burst-mode regime. This laser system generates 145 W, 13 ps pulses directly from the fiber, which is the highest average power for ultrafast burst-mode operation, to the best of our knowledge.

REFERENCES

1. M. E. Fermann and I. Hartl, "Ultrafast fibre lasers," Nat. Photonics **7**, 868–874 (2013).
2. C. Jauregui, J. Limpert, and A. Tünnermann, "High-power fibre lasers," Nat. Photonics **7**, 861–867 (2013).
3. K. Sugioka and Y. Cheng, *Ultrafast Laser Processing: From Micro-To Nanoscale*, 1st ed. (Pan Stanford, 2013).
4. M. Lenzner, J. Kraeger, W. Kautek, and F. Krausz, "Precision laser ablation of dielectrics in the 10-fs regime," Appl. Phys. A **68**, 369–371 (1999).
5. R. Srinivasan and B. Braren, "Ultraviolet laser ablation of organic polymers," Chem. Rev. **89**, 1303–1316 (1989).
6. E. G. Gamaly and A. V. Rode, "Physics of ultra-short laser interaction with matter: from phonon excitation to ultimate transformations," Prog. Quantum Electron. **37**, 215–323 (2013).
7. A. Ancona, S. Doring, C. Jauregui, F. Roser, J. Limpert, S. Nolte, and A. Tünnermann, "Femtosecond and picosecond laser drilling of metals at high repetition rates and average powers," Opt. Lett. **34**, 3304–3306 (2009).
8. M. Lapczyna, K. P. Chen, P. R. Herman, H. W. Tan, and R. S. Marjoribanks, "Ultra high repetition rate (133 MHz) laser ablation of aluminum with 1.2-ps pulses," Appl. Phys. A **69**, S883–S886 (1999).
9. W. Hu, Y. C. Shin, and G. King, "Modeling of multi-burst mode picosecond laser ablation for improved material removal rate," App. Phys. A **98**, 407–415 (2010).

10. H. Kalaycıoğlu, K. Eken, and F. Ö. Ilday, "Fiber amplification of pulse bursts up to 20 μJ pulse energy at 1 kHz repetition rate," Opt. Lett. **36**, 3383–3385 (2011).

11. H. Kalaycıoğlu, Y. B. Eldeniz, Ö. Akçaalan, S. Yavas, K. Gurel, M. Efe, and F. Ö. Ilday, "1-mJ pulse bursts from a Yb-doped fiber amplifier," Opt. Lett. **37**, 2586–2588 (2012).

12. H. Kalaycıoğlu, Ö. Akçaalan, S. Yavas, Y. B. Eldeniz, and F. Ö. Ilday, "A burst-mode Yb-doped fiber amplifier system optimized for low-repetition-rate operation," J. Opt. Soc. Am. B **32**, 900–906 (2015).

13. S. Breitkopf, A. Klenke, T. Gottschall, H. J. Otto, C. Jauregui, J. Limpert, and A. Tünnermann, "58 mJ burst comprising ultrashort pulses with homogenous energy level from an Yb-doped fiber amplifier," Opt. Lett. **37**, 5169–5171 (2012).

14. D. M. Baney, P. Gallion, and R. S. Tucker, "Theory and measurement techniques for the noise figure of optical amplifiers," Opt. Fiber Technol. **6**, 122–154 (2000).

15. P. Elahi, S. Yılmaz, Y. B. Eldeniz, and F. Ö. Ilday, "Generation of picosecond pulses directly from a 100 W, burst-mode, doping-managed Yb-doped fiber amplifier," Opt. Lett. **39**, 236–239 (2014).

16. A. Chong, J. Buckley, W. Renninger, and F. W. Wise, "All-normal-dispersion femtosecond fiber laser," Opt. Express **14**, 10095–10100 (2006).

17. P. Elahi, S. Yılmaz, Ö. Akçaalan, H. Kalaycıoğlu, B. Öktem, C. Senel, F. Ö. Ilday, and K. Eken, "Doping management for high-power fiber lasers: 100-W, few-ps pulse generation from an all-fiber-integrated amplifier," Opt. Lett. **37**, 3042–3044 (2012).

18. P. K. Mukhopadhyay, K. Özgören, I. L. Budunoglu, and F. Ö. Ilday, "All-fiber low-noise high-power femtosecond Yb-fiber amplifier system seeded by an all-normal dispersion fiber oscillator," IEEE J. Sel. Top. Quantum **15**, 145–152 (2009).

19. I. Pavlov, E. Dülgergil, E. Ilbey, and F. Ö. Ilday, "Diffraction-limited, 10-W, 5-ns, 100-kHz, all-fiber laser at 1.55 μm," Opt. Lett. **39**, 2695–2698 (2014).

20. J. W. Nicholson, J. Jasapara, W. Rudolph, F. G. Omenetto, and A. J. Taylor, "Full-field characterization of femtosecond pulses by spectrum and cross-correlation measurements," Opt. Lett. **24**, 1774–1776 (1999).